Porphyrin-based metallopolymers: synthesis, characterization and pyrolytic study for the generation of magnetic metal nanoparticles

Qingchen Dong,*a Wenshan Qu,b Wenqing Liang,a Feifei Tai,a Kunpeng Guo,a Chi-Wah Leung,c Yih Hsing Lo*d and Wai-Yeung Wong*ae

* Corresponding authors

a MOE Key Laboratory for Interface Science and Engineering in Advanced Materials and Research Center of Advanced Materials Science and Technology, Taiyuan University of Technology, 79 Yingze West Street, Taiyuan 030024, P. R. China

E-mail: dongqingchen@tyut.edu.cn

b Institute of Carbon Materials Science, Shanxi Datong University, Datong 037009, P. R. China

c Department of Applied Physics, The Hong Kong Polytechnic University, Hung Hom, Hong Kong, P. R. China

E-mail: dennis.leung@polyu.edu.hk

d Department of Applied Physics and Chemistry, University of Taipei, Taipei 100, Taiwan

E-mail: yhlo@utaipei.edu.tw

e Institute of Molecular Functional Materials, Department of Chemistry and Partner State Key Laboratory of Environmental and Biological Analysis, Hong Kong Baptist University, Waterloo Road, Kowloon Tong, Hong Kong, P. R. China

E-mail: rwywong@hkbu.edu.hk

Abstract

Metallopolymers with different metal centers, pendant groups and linkages exhibit diverse structures and properties, thus giving rise to versatile applications, *e.g.*, as emissive and photovoltaic materials, optical limiters, materials for nano-electronics, information storage, nanopatterning and sensing, macromolecular catalysts and artificial enzymes, and stimuli-responsive materials. Recently, metallopolymers as precursors to generate monometallic or metal alloy nanoparticles are of great interest owing to their advantages of ease of processability, atomic level mixing, and stoichiometric control over composition. By taking advantage of the template effect of porphyrin compounds, a series of monometallic and heterobimetallic polymers are synthesized which are characterized by NMR, IR, HRMS, EA, GPC and TGA, respectively. Photophysical properties of these metallopolymers are also studied by UV-vis spectroscopy. Pyrolytic treatment of these metallopolymers generates various magnetic monometallic and metal alloy nanoparticles which can be used in data storage, catalysis, biomedicine, *etc.*

Introduction

Metallopolymers have attracted intense and increasing research interest over the last two decades[1–5] and are of growing importance in many practical applications, *e.g.* as photovoltaic cells,[6] nanocomposites,[7,8] biosensors,[9] and polymer light-emitting diodes.[10,11] In recent years, owing to the ability of metallopolymers to be easily processed and fabricated into thin films, fibers and other forms, researchers have attempted to synthesize metal NPs and metal alloy NPs by utilizing metallopolymers as templates which, on pyrolysis or photolysis, generate NPs with a narrow size distribution and a precisely controllable composition as well as density per unit area.[12–18] Previously, our groups reported a one-pot method to directly synthesize $L1_0$ FePt alloy NPs through the pyrolysis of a metallopolymer containing both Fe and Pt atoms without any post-treatments.[19,20] In particular, by combining the merits of nanoimprint lithography and solution-processability of the new metallopolymer we reported that the $L1_0$ FePt-based bit patterned media with an areal density of 2.58 Gb in^{-2} were accomplished quickly in a large area at a relatively low cost.[20] More recently, we also investigated the influence of pyrolysis temperature on the size and magnetic properties of the resulting ferromagnetic alloy NPs in detail.[21] Porphyrins which are heterocyclic macrocycles composed of four modified pyrrole subunits have been widely studied and utilized for more than one century for diverse applications.[22–27] Since the synthesis of the parent and the simplest porphyrin, namely porphine, more and more modified porphyrins with various properties have already been explored and applied in the practical life. For example, metalloporphyrins are among the most effective optical limiters[22] and biological oxygen sensors,[23,24] and bisporphyrins with various kinds of linkages and different central metal ions are potentially applicable in host–guest chemistry, chemical sensing, supramolecular chirogenesis, catalytic photooxidation, molecular switches,

photoinduced energy transfer, two-photon absorption, *etc.*[25–27] In this work, by taking advantage of the template effect of porphyrin compounds, we report the synthesis of a series of new porphyrin-based heterobimetallic and mononuclear metallopolymers, followed by a one-step generation of monometallic and metal alloy NPs by pyrolyzing the as-synthesized metallopolymers, which have great application perspectives in data recording systems, optoelectronic devices, catalysis, biomedicine, *etc.*

Results and discussion

Synthesis and characterization of target metallopolymers

Synthesis of the target metallopolymers was performed *via* the Sonogashira coupling reaction which gave the macromolecular products almost quantitatively.[28] Scheme 1 shows the detailed synthetic routes of the heterobimetallic or mononuclear metallopolymers. The diethynyl ligands incorporating porphyrin moieties were prepared first. To begin with, an aromatic aldehyde derivative was prepared from 4-bromobenzaldehyde according to the pathway shown in Scheme 1. 4-(2-(Trimethylsilyl)ethynyl)benzaldehyde was easily prepared through the Sonogashira coupling reaction from 4-bromobenzaldehyde and trimethylsilylacetylene in triethylamine using $Pd(PPh_3)_4$ and CuI as catalysts. The *meso*-phenyldipyrromethane was prepared *via* the acid-catalyzed condensation of pyrrole and benzaldehyde using an excessive amount of pyrrole as the solvent. Then the key *trans*-substituted porphyrin ligand precursor was synthesized by the acid-catalyzed condensation of *meso*-phenyldipyrromethane with the aromatic aldehyde derivatives, followed by oxidation with 2,3-dichloro-5,6-dicyano-1,4-benzoquinone (DDQ) at room temperature. Finally, the trimethylsilyl group (TMS) was easily removed in the presence of

potassium carbonate in methanol and dichloromethane at room temperature to give the free base porphyrin ligand with diethynyl terminal groups.

After the key intermediate compound was obtained, the *trans*-substituted free base porphyrin was allowed to coordinate with anhydrous $FeCl_3$, $Co(OAc)_2$, $Cu(OAc)_2$ and $Ni(OAc)_2$, to give rise to the diethynyl Fe(III), Co(II), Cu(II) and Ni(II) porphyrin complexes, which were denoted DETPP-Fe, DETPP-Co, DETPP-Cu and DETPP-Ni, respectively. Then, the coordinated Pt(II) dichloride complex was used to couple with the diethynyl Fe(II) porphyrin through the copper(I)-catalyzed dehydrohalogenation reaction to form the FePt-containing metallopolymers (denoted DETPP-P-FePt). Next, the diethynyl Cu(II) and Ni(II) porphyrin were allowed to react with the ferrocene-containing diiodide complexes, respectively, to generate the corresponding FeCu- and FeNi-containing metallopolymers (denoted DETPP-P-FeCu and DETPP-P-FeNi). Then, the Fe(III), Co(II) and Ni(II) porphyrin complexes were allowed to react with a diiodofluorene compound through the Sonogashira coupling reaction to generate the Fe-, Co- and Ni-containing metallopolymers (denoted DETPP-P-Fe, DETPP-P-Co and DETPP-P-Ni), respectively. All these polymerization reactions proceeded with satisfactory yields and the products were purified by repeated precipitation in a minimum volume of dichloromethane from methanol 2–3 times. The resulting polymers were characterized by NMR, EA, IR, GPC and TGA.

Photophysical properties of the as-synthesized heterobimetallic polymers

The photophysical properties of the porphyrin ligands and porphyrin-based heterobimetallic polymers have been studied by UV-vis spectroscopy. The overlap plot of the normalized optical absorption spectra in dilute CH_2Cl_2 solution is shown in Fig. 1. As shown in the absorption spectra, before complexation with the metal ion, diethynyl porphyrin (DETPP) exhibits a strong

Soret band at *ca.* 420 nm and four weak Q-bands at 450 nm, 515 nm, 550 nm and 590 nm, respectively, which is a typical absorption profile of porphyrin compounds.[29,30] However, after complexation, each polymer exhibits a strong Soret band at *ca.* 418 nm ($\pi \rightarrow \pi^*$ transition, $S_0 \rightarrow S_2$) and only one weak Q-band at around 540 nm ($\pi \rightarrow \pi^*$ transition, $S_0 \rightarrow S_1$). These two sets of peaks are clearer than those in DETPP due to the exciton coupling, which is common in linear oligomers and polymers of porphyrins. It should be noted that, in the spectrum of DETPP-P-Co, a new and strong absorption peak at 434 nm emerged. This may be attributed to the formation of dimeric species due to the metal–metal interaction resulting from the nonplanar configuration of the Co-porphyrin, which has been further verified by the concentration-dependent UV-vis absorption spectra of DETPP-P-Co in dichloromethane (see Fig. S1 in ESI†).

Pyrolysis of metallopolymers

Pyrolysis experiments of the as-synthesized metallopolymers were performed similar to the procedure reported before by our group, that is the metallopolymer was placed in a ceramic boat, which was then allowed to be put in a tube furnace and underwent pyrolytic treatment for 1 h in an argon atmosphere with the heating rate of 20 °C min^{-1} at 800 °C. Then the tube furnace was allowed to cool down to ambient temperature. The NPs synthesized by pyrolysis of metallopolymers were denoted NP-Fe, NP-Co, NP-Ni, NP-FePt, NP-FeNi and NP-FeCu, respectively, according to the metallic centers of the corresponding mononuclear and heterobimetallic polymers.

Characterization of the as-synthesized metallic NPs

In order to identify the compositions and phases of the resulting NPs generated from the pyrolysis of metallopolymers, powder X-ray diffraction (PXRD) measurements were performed. Fig. 2 shows the PXRD patterns of NP-Fe, NP-Co, NP-Ni, NP-FePt, NP-FeNi and NP-FeCu, respectively, and all the peaks in each of the PXRD patterns have been assigned. As we can see from Fig. 2(a–c), all the monometallic NPs exhibit a PXRD pattern with sharp peaks, implying that these NPs have good crystallinity. By comparison with the PXRD pattern in the database (JCPDS no. 52-0513, 15-0806 and 45-1027), NP-Fe and NP-Co are confirmed to be fcc-structured NPs, while NP-Ni is composed of simple cubic structured NPs. Fig. 2(d–f) show the PXRD pattern of the as-synthesized metal alloy NPs, namely, NP-FePt, NP-FeNi and NP-FeCu. All the PXRD patterns of metal alloy NPs display relatively broad peaks, demonstrating that the crystallinity of metal alloy NPs is not as good as those monometallic NPs. Fig. 2(d) shows the PXRD pattern of the NP-FePt nanomaterial, in which each peak was recognized. From this pattern, (001) and (110) peaks which are the characteristic peaks of $L1_0$ phase FePt alloy NPs can be clearly observed at ~22° and ~33°.[31] Besides, no Fe_xN_y and Pt_xN_y phases are observed in this PXRD pattern. As depicted in Fig. 2(e), the labeled peaks correspond to the fcc FeNi alloy NPs (JCPDS no. 18-0877), while asterisks correspond to the oxidized components.[32,33] Thus compared to the FePt alloy NPs, the chemical stability of FeNi alloy NPs decreased due to the absence of the spin–orbit coupling and hybridization of 3d and 5d electrons. Fig. 2(f) shows the PXRD pattern of NP-FeCu nanomaterial (JCPDS no. 49-1399), in which the diffraction peaks are broader than NP-FePt and NP-FeNi, manifesting the worst crystallinity of FeCu alloy NPs. The composition of the as-synthesized binary metal alloy NPs was verified through the analysis of energy-dispersive X-ray (EDX) measurements. The EDX

results indicate that the ratio of Fe and Pt in NP-FePt is approximately 1 : 1 as expected for $L1_0$ phase FePt NPs. This is in close agreement with the composition as inferred from the (111) peak in the PXRD pattern, and is also consistent with the stoichiometry of the metallopolymer with the nearly equal atomic ratio of Fe and Pt. However, for NP-FeCu and NP-FeNi, the atomic ratios of Ni : Fe and Cu : Fe are close to 5 : 1 and 3 : 1, respectively. Thus, it has been shown experimentally that the absence of spin–orbit coupling and hybridization of Fe 3d and Pt 5d electrons can significantly influence the degree of alloying of the two metallic elements, as well as the composition, structure and magnetic properties of the resulting alloy NPs. Morphologies of the resulting metallic NPs were investigated by transmission electron microscopy (TEM), as shown in Fig. 3. It can be seen clearly that all of the resulting metallic NPs were embedded in a carbonaceous matrix and exhibited spherical morphology. Investigation of the particle size and size distribution of the NPs was also performed by analysis of the corresponding TEM images. It turns out that the average NP sizes of NP-Fe, NP-Co, NP-Ni, NP-FePt, NP-FeNi and NP-FeCu are 11.8, 13.2, 15.7, 11.5, 18.2 and 19.2 nm, respectively, with relatively broad size distributions (standard deviation of *ca.* 13, 10, 15, 11, 22 and 24%). It should be noted that NP-FeNi and NP-FeCu have a larger size and standard deviation as compared to NP-FePt, which could also be attributed to the absence of the spin–orbit coupling and hybridization of 3d and 5d electrons, and thus the poor diffusion of Fe into Ni and Cu nuclei to form metal alloy NPs.

Magnetic properties of the as-synthesized NPs

Magnetic hysteresis loops recorded for the as-prepared bulk Fe, Co and Ni NPs as powder at 300 K are shown in Fig. 4(a). It can be clearly seen that all the monometallic NPs exhibit superparamagnetic behaviours, as exhibited by the vanishingly small coercivity and remanent

magnetization. The saturation magnetization of these NPs is much smaller than that of the bulk. The M–H loops of the resulting $L1_0$ FePt NPs as powder at 300 K and 5 K are shown in Fig. 4(b). We can learn from Fig. 4(b) that the coercivity (H_c, an indicator of magnetocrystalline anisotropy) of $L1_0$ FePt NPs at 300 K is 0.54 T, which is satisfactory for practical magnetic data storage at room temperature because the data can be manipulated easily by an external magnetic field with a magnetic field strength achievable in typical magnetic data storage systems. The coercivity at low temperature increased dramatically, which can reach as high as 1.12 T. The ultra-small averaged diameter and ultra-high coercivity of the resulting $L1_0$ FePt NPs at low temperature render them great potential for use in quantum computation systems.[34]

Conclusions

We have presented the synthesis of a series of porphyrin-based heterobimetallic or mononuclear metallopolymers. By taking these metallopolymers as precursors, various monometallic and metal alloy NPs were synthesized, especially for ferromagnetic $L1_0$ phase FePt NPs which were generated in a single step without any post-annealing treatment as reported previously. The TEM images indicate that the resulting metallic NPs are spherical NPs within a carbonaceous matrix which could immobilize and protect these magnetic NPs. Magnetic properties of the resulting Fe, Co, Ni and FePt NPs were also investigated by VSM measurements, which suggest that all the as-synthesized monometallic NPs are superparamagnetic, while FePt NPs are ferromagnetic with coercivity values of 0.54 T at room temperature and 1.12 T at low temperature, manifesting that the FePt-containing polymer can be used as a precursor for the fabrication of FePt-based bit-

patterned-media for data storage. In the future work, we will try to explore the application of these carbon/metal NPs in catalysis or biosensing.

Experimental

General information

All reactions were carried out under nitrogen unless otherwise stated. Commercially available reagents were used as received without further purification. [$PtCl_2$(^{n}Non_2bipy)] and 2,7-diiodo-9,9-dihexadecylfluorene were synthesized according to the method as reported previously.[19,35] All reactions were monitored by thin-layer chromatography (TLC) using Merck pre-coated glass plates. The compounds were visualized under UV light at 254 and 365 nm. Separation or purification of products was achieved by column chromatography or preparative TLC using silica gel from Merck (230–400 mesh). NMR spectra were measured in $CDCl_3$ on a Bruker AV 400 NMR instrument with chemical shifts being referenced against tetramethylsilane as the internal standard for ^{1}H and ^{13}C NMR data. IR spectra were recorded on the Nicolet Magna 550 Series II FTIR spectrometer using KBr pellets for solid state spectroscopy. The positive-ion fast atom bombardment (FAB) mass spectra were recorded in the *m*-nitrobenzyl alcohol matrix on a Finnigan-MAT SSQ710 mass spectrometer. Thermal analyses were performed using a Perkin-Elmer TGA 6 thermal analyzer. The molecular weight of the polymer was determined by GPC using a HP 1050 series HPLC equipped with visible wavelength and fluorescent detectors against polystyrene standards.

Preparation of 4-(2-(trimethylsilyl)ethynyl)benzaldehyde

To an ice-cooled solution of 4-bromobenzaldehyde (1.513 g, 8.22 mmol) in freshly distilled triethylamine (30 mL) was added CuI (78 mg) and $Pd(PPh_3)_4$ (280 mg). After the solution was stirred for 30 min at 0 °C, trimethylsilylacetylene (2.3 mL, 16.32 mmol) was then added and the mixture was stirred for 30 min in an ice-bath before being warmed to room temperature. After reacting for 30 min at room temperature, the mixture was heated to 50 °C for 12 h. The solution was then allowed to cool to room temperature and the solvent mixture was evaporated *in vacuo*. The crude product was purified by column chromatography on silica gel using CH_2Cl_2/hexane (1 : 1, v/v) as an eluent to provide the target product as a pale-yellow solid (1.81 g, 78%). ^{1}H NMR ($CDCl_3$, 400 MHz, δ/ppm): 10.00 (s, 1H, C*H*O), 7.83 (m, 2H, Ar–*H*), 7.61 (d, J = 8.0 Hz, 2H, Ar–*H*), 0.27 (s, 9H, TMS); ^{13}C NMR ($CDCl_3$, 125 MHz, δ/ppm): 191.71 (CHO), 135.74, 132.68, 129.66, 129.54, 104.01 (Ar), 99.24, 77.45 (C≡C), 0.28 (TMS).

Preparation of *meso*-phenyldipyrromethane

A solution of benzaldehyde (0.1 mL, 1 mmol) and pyrrole (2.8 mL, 40 mmol) was degassed by bubbling with argon for 10 min, and then trifluoroacetic acid (8 μL, 0.1 mmol) was added. The solution was stirred for 15 min at room temperature, at which point no starting aldehyde was shown by TLC analysis. The mixture was diluted with CH_2Cl_2 (50 mL), then washed with 0.1 N aq. NaOH and water, and dried over anhydrous sodium sulfate. The solvent was removed under reduced pressure and then the unreacted pyrrole was removed by vacuum distillation at room temperature. The resulting yellow amorphous solid was dissolved in a minimal quantity of the eluent and was purified by column chromatography on silica gel eluting with hexane/ethyl acetate/triethylamine (80 : 20 : 1, v/v/v) to give *meso*-phenyldipyrromethane as a pale-brown

solid (92 mg, 39%). ^{1}H NMR ($CDCl_3$, 400 MHz, δ/ppm): 7.93 (m, 2H, Ar–*H*), 7.31 (d, J = 4.8 Hz, 2H, Ar–*H*), 7.23 (m, 2H, Ar–*H*), 6.70 (d, J = 1.2 Hz, 2H, Ar–*H*), 6.16 (d, J = 3.0 Hz, 2H, Ar–*H*), 5.92 (d, J = 0.4 Hz, 2H, Fc–*H*), 5.48 (d, 1H, Fc–*H*); ^{13}C NMR ($CDCl_3$, 125 MHz, δ/ppm): 142.09, 132.55, 128.68, 128.44, 127.02, 117.30, 108.43, 107.27 (Ar), 43.96 (CH).

Preparation of DETPP-TMS

A solution of 4-(2-trimethylsilylethynyl)benzaldehyde (421 mg, 1.48 mmol) and *meso*-phenyldipyrromethane (350 mg, 1.48 mmol) in CH_2Cl_2 (100 mL) was purged with nitrogen for 30 min, and then trifluoroacetic acid (TFA) (118 mg, 1.04 mmol) was added. The mixture was stirred for 3 h at room temperature, and then DDQ (680 mg, 2.96 mmol) was added. After the mixture was stirred at room temperature for an additional 30 min, the reaction was quenched by adding triethylamine (2 mL). The solvent was removed, and the residue was purified by flash column chromatography on silica gel using CH_2Cl_2/hexane (1 : 1, v/v) as the eluent. Recrystallization from CH_2Cl_2/methanol gave DETPP-TMS as a purple solid (233 mg, 39%). ^{1}H NMR ($CDCl_3$, 400 MHz, δ/ppm): 8.81 (d, 8H, J = 8.0 Hz, Ar–*H*), 8.18 (m, 8H, Ar–*H*), 7.86 (d, J = 8.0 Hz, 4H, C=C*H*), 7.73 (d, J = 8.0 Hz, 6H, Ar–*H*), 0.38 (s, 18H, TMS), −2.80 (t, J = 8.0 Hz, 2H, N–*H*); ^{13}C NMR ($CDCl_3$, 125 MHz, δ/ppm): 142.34, 142.31, 142.24, 141.98, 141.90, 134.42, 134.32, 130.26, 127.70, 127.65, 126.63, 122.55, 122.50, 122.48, 120.41, 120.31, 120.18, 119.39, 119.25, 104.90, 104.87, 95.54, 95.49 (Ar).

Preparation of DETPP

A mixture of DETPP-TMS (100 mg, 0.13 mmol) and K_2CO_3 (38 mg, 0.27 mmol) in methanol (20 mL) and CH_2Cl_2 (30 mL) solution mixture was stirred overnight under a nitrogen atmosphere

at room temperature. The completion of the reaction was verified by spot TLC. The solvent was removed by rotary evaporation. The resulting mixture was redissolved in CH_2Cl_2 (50 mL) and washed with three portions of 20 mL water. The light yellow organic phase was dried over anhydrous sodium sulfate and evaporated to dryness. The crude product was purified by column chromatography on silica gel eluting with CH_2Cl_2/hexane (1 : 2, v/v) to provide DETPP as a pale-yellow solid (80 mg, 93%). ^{1}H NMR ($CDCl_3$, 400 MHz, δ/ppm): 8.82 (m, 8H, Ar–*H*), 8.19 (m, 8H, Ar–*H*), 7.90–7.75 (m, 10H, Ar–*H*), 3.31 (s, 2H, C≡C–*H*), −2.81 (s, 2H, N–*H*); ^{13}C NMR ($CDCl_3$, 125 MHz, δ/ppm): 142.76, 142.07, 141.97, 134.54, 130.52, 127.81, 127.75, 126.73, 121.64, 120.57, 120.45, 120.29, 119.20,119.08 (Ar), 83.64, 76.69 (C≡C). IR (KBr): 3284 (ν_C≡C–H) cm^{-1}; 2108 (ν_C≡C) cm^{-1}.

Preparation of DETPP-Fe

To a solution of the DETPP compound (70 mg, 0.097 mmol) in absolute ethanol (20 mL) was added a solution of anhydrous $FeCl_3$ (15 mg, 0.12 mmol) in ethanol (3 mL). The reaction mixture was stirred at reflux for 4 h. Then the hot solution was filtered, washed with water and dried under vacuum to give ppy-Fe as a brown solid (43 mg, 57%). ^{1}H NMR ($CDCl_3$, 400 MHz, δ/ppm): 8.83 (m, 8H, Ar–*H*), 8.18 (m, 8H, Ar–*H*), 7.87 (d, *J* = 8.0 Hz, 4H, Ar–*H*), 7.76 (d, *J* = 8.0 Hz, 6H, Ar–*H*), 2.95, 2.88 (d, *J* = 28 Hz, 2H, C≡C–*H*). HRMS (ESI, *m*/*z*): [M + H]$^+$ calcd for $C_{48}H_{28}ClFeN_4$, 751.1352, found, 751.1531. Anal. calcd for $C_{48}H_{28}ClFeN_4$: C, 75.67; H, 3.75; N, 7.45. Found: C, 75.97; H, 3.71; N, 7.27. IR (KBr): 3284 (ν_C≡C–H) cm^{-1}; 2103 (ν_C ≡C) cm^{-1}.

Preparation of DETPP-Co

In a 250 mL distillation flask, DETPP (36 mg, 0.055 mmol) and NaOAc (20.5 mg, 0.25 mmol) were stirred in 75 mL chlorobenzene and 50 mL DMF. After the addition of two equivalents of $Co(OAc)_2$ (15.5 mg, 0.11 mmol), a Soxhlet extractor with a cellulose filter thimble filled with 3 g of K_2CO_3 was attached to the distillation flask. The assembly was completed with a condenser on the top of the extractor; and then the mixture was heated to reflux at 150 °C overnight. The extent of the reaction was monitored by TLC or UV-Vis spectroscopy until all the TPP-DE was consumed. After the reaction was complete, the solvent was removed under vacuum. The remaining solid was dissolved in 150 mL chloroform, and washed with water. The organic layer was further washed with a saturated sodium bicarbonate solution, and then dried over anhydrous K_2SO_4. After evaporation of the solvent, the solid was recrystallized from chloroform/heptane. A pink-purple crystalline solid was collected. Yield: (12 mg, 30%). IR (KBr): 3294 ($\nu_{C\equiv C}$–H) cm^{-1}; 2107 ($\nu_{C\equiv C}$) cm^{-1}. HRMS (ESI, *m*/*z*): $[M + H]^+$ calcd for $C_{48}H_{28}CoN_4$, 719.1646, found, 719.1638. Anal. calcd for $C_{48}H_{28}CoN_4$: C, 80.11; H, 3.92; N, 7.78. Found: C, 80.03; H, 3.69; N, 7.72.

Preparation of DETPP-Ni

To a solution of the DETPP compound (40 mg, 0.055 mmol) in chloroform (20 mL) was added a solution of $Ni(OAc)_2{\cdot}4H_2O$ (14 mg, 0.057 mmol) in ethanol (5 mL). The reaction mixture was stirred at reflux overnight. Afterwards the solvent was removed, and the crude product was purified by column chromatography to afford DETPP-Ni as a red solid (39 mg, 75%). ^{1}H NMR ($CDCl_3$, 400 MHz, δ/ppm): 8.75 (m, 8H, Ar–*H*), 7.99 (t, *J* = 8.0 Hz, 8H, Ar–*H*), 7.81 (d, *J* = 8.0 Hz, 4H, Ar–*H*), 7.68 (d, *J* = 8.0 Hz, 6H, C=C*H*), 3.27 (s, 2H, C≡C–*H*). HRMS (ESI, *m*/*z*): [M +

H]$^+$ calcd for $C_{48}H_{28}NiN_4$, 718.1667, found, 718.1712. Anal. calcd for $C_{48}H_{28}NiN_4$: C, 80.13; H, 3.92; N, 7.79. Found: C, 79.98; H, 3.80; N, 7.65.IR (KBr): 3289 ($\nu_C{\equiv}C$–H) cm^{-1}; 2112 ($\nu_C{\equiv}C$) cm^{-1}.

Preparation of DETPP-Cu

To a solution of the DETPP compound (30 mg, 0.045 mmol) in $CHCl_3$ (20 mL) and ethanol (20 mL) was added anhydrous $Cu(OAc)_2$ (82 mg, 0.45 mmol). The reaction mixture was stirred at room temperature for 3 h. After evaporation of the solvent, the crude product was purified by column chromatography to give DETPP-Cu as a red solid (33 mg, 87%). ^{1}H NMR ($CDCl_3$, 600 MHz, δ/ppm): 8.85 (m, 8H, Ar–*H*), 8.02 (m, 8H, Ar–*H*), 7.90 (d, J = 7.2 Hz, 4H, Ar–*H*), 7.76 (d, J = 7.2 Hz, 6H, Ar–*H*), 3.32 (s, 2H, C≡C–*H*). HRMS (ESI, *m*/*z*): [M + H]$^+$ calcd for $C_{48}H_{28}CuN_4$, 723.1610, found, 723.1630. Anal. calcd for $C_{48}H_{28}CuN_4$: C, 79.60; H, 3.90; N, 7.74. Found: C, 78.89; H, 3.77; N, 7.39.IR (KBr): 3295 ($\nu_C{\equiv}C$–H) cm^{-1}; 2108 ($\nu_C{\equiv}C$) cm^{-1}.

Preparation of DETPP-P-Fe, DETPP-P-Co and DETPP-P-Ni

Since the two Fe-, Co- and Ni-containing metallopolymers were prepared by a similar procedure, the general procedure for this copper(I)-catalyzed dehydrohalogenation reaction is illustrated here for the preparation of DETPP-P-Fe. A mixture of DETPP-Fe (43 mg, 0.057 mmol) and 2,7-diiodo-9,9-dihexadecylfluorene (50 mg, 0.057 mmol) was dissolved in NEt_3/CH_2Cl_2 (30 mL, 4 : 1 v/v), followed by the addition of CuI (10 mg). The red solution was stirred overnight under a nitrogen atmosphere at room temperature. The solvent was removed and the mixture was redissolved in a small amount of CH_2Cl_2. The solution was filtered and methanol (30 mL) was then added into the filtrate to allow the precipitation of the polymer. The product was collected

as a red solid (29.1 mg, 41.2%). ^{1}H NMR ($CDCl_3$, 600 MHz, δ/ppm) for DETPP-P-Fe: 8.83 (s, 8H, Ar–*H*), 8.44 (d, *J* = 8.4 Hz, 3H, Ar–*H*), 8.31 (d, *J* = 8.4 Hz, 3H, Ar–*H*), 7.88 (d, *J* = 7.8 Hz, 8H, Ar–*H*), 6.13 (d, *J* = 8.4 Hz, 2H, Ar–*H*), 1.25 (m, 60H, C*H*$_2$), 0.88 (t, 6H, C*H*$_3$); ^{1}H NMR ($CDCl_3$, 600 MHz, δ/ppm) for DETPP-P-Ni: 8.77 (m, 8H, Ar–*H*), 8.19 (m, 8H, Ar–*H*), 7.85 (d, *J* = 7.8 Hz, 4H, Ar–*H*), 7.71 (d, *J* = 7.2 Hz, 6H, Ar–*H*), 7.67 (t, 4H, Ar–*H*), 7.43 (d, *J* = 7.8 Hz, 2H, Ar–*H*), 1.90 (t, 4H, C*H*$_2$), 1.27 (m, 54H, C*H*$_2$), 0.90 (t, 6H, C*H*$_3$). Anal. calcd for $(C_{93}H_{98}ClFeN_4)_n$: C, 81.95; H, 7.25; N, 4.11. Found: C, 81.33; H, 7.06; N, 3.95; anal. calcd for $(C_{93}H_{98}CoN_4)_n$: C, 83.94; H, 7.42; N, 4.21. Found: C, 83.62; H, 7.05; N, 4.01; anal. calcd for $(C_{93}H_{98}NiN_4)_n$: C, 83.95; H, 7.42; N, 4.21. Found: C, 83.16; H, 7.09; N, 4.19.IR (KBr): 2151 ($\nu_C\equiv C$) cm^{-1} for DETPP-P-Fe, 2124 ($\nu_C\equiv C$) cm^{-1} for DETPP-P-Co and 2108 ($\nu_C\equiv C$) cm^{-1} for DETPP-P-Ni. GPC (THF): M_w = 19 640, M_n = 11 630, M_w/M_n = 1.69 for DETPP-P-Fe, M_w = 10 468, M_n = 5199, M_w/M_n = 2.01 for DETPP-P-Co, M_w = 7243, M_n = 6177, M_w/M_n = 1.17 for DETPP-P-Ni. T_{decomp} (°C): 434 °C for DETPP-P-Fe, 322 °C for DETPP-P-Co, 425 °C for DETPP-P-Ni.

Preparation of DETPP-P-FePt

To a solution of DETPP-Fe (43 mg, 0.057 mmol) in 30 mL of dichloromethane/triethylamine (1 : 1, v/v) was added the [$PtCl_2$(^{n}Non$_2$bipy)] (38 mg, 0.057 mmol) compound and copper iodide (5 mg). The mixture was allowed to stir at room temperature overnight under a nitrogen atmosphere. Afterwards the solvent was removed and the mixture was redissolved in a small amount of CH_2Cl_2 and reprecipitated with the addition of methanol. Centrifugation was done to give a residual solid. The porphyrin-based heterobimetallic polymer DETPP-P-FePt was isolated as a red solid (73 mg, 91%). Anal. calcd for $(C_{76}H_{70}ClFePtN_6)_n$: C, 67.43; H, 5.21; N, 6.21.

Found: C, 67.53; H, 5.10; N, 6.05.IR (KBr): 2113 ($\nu_{C\equiv C}$) cm^{-1}. GPC (THF): M_w = 4824, M_n = 4571, M_w/M_n = 1.06. T_{decomp} (°C): 304 °C.

Preparation of DETPP-P-FeCu

A mixture of DETPP-Cu (45 mg, 0.062 mmol) and 1,1′-diiodoferrocene (40 mg, 0.062 mmol) was dissolved in NEt_3/THF (30 mL, 4 : 1 v/v), followed by the addition of CuI (5 mg) and $Pd(PPh_3)_4$ (8 mg). The red solution was stirred overnight under a nitrogen atmosphere at room temperature. The solvent was removed and the mixture was redissolved in a small amount of CH_2Cl_2. The solution was filtered and methanol (30 ml) was added to the filtrate to allow the precipitation of the polymer. The product was collected as a dark red solid (60 mg, 82%). Anal. calcd for $(C_{72}H_{42}FeCuN_4)_n$: C, 79.88; H, 3.91; N, 5.18. Found: C, 79.59; H, 3.81; N, 5.03. IR (KBr): 2155 ($\nu_{C\equiv C}$) cm^{-1}. GPC (THF): M_w = 10 861, M_n = 9619, M_w/M_n = 1.13. T_{decomp} (°C): 236 °C.

Preparation of DETPP-P-FeNi

The procedure for the preparation of DETPP-P-FeNi was similar to that of DETPP-P-FeCu. The resulting product was obtained as a red solid (42 mg, 89%). Anal. calcd for $(C_{72}H_{42}FeNiN_4)_n$: C, 80.24; H, 3.93; N, 5.20. Found: C, 79.65; H, 3.22; N, 4.96.IR (KBr): 2100 ($\nu_{C\equiv C}$) cm^{-1}. GPC (THF): M_w = 5533, M_n = 4449, M_w/M_n = 1.24. T_{decomp} (°C): 302 °C.

Pyrolysis of metallopolymers

The as-synthesized metallopolymer was put in a ceramic boat, which was then placed inside a quartz reaction tube equipped with temperature and gas-flow controls. Then, the whole set-up was heated up to the desired temperature at a rate of 20 °C min^{-1} under an argon atmosphere.

Nanoparticle characterization

Structural characterization of the as-synthesized NPs was performed by PXRD on a Bruker AXS D8 Advance X-ray diffractometer machine, using $CuK_{\alpha 1}$ (λ = 540 nm, 40 kV, dan 40 mA) for analyzing the composition and phase purity of the resulting NPs. TEM was performed using a Tecnai G2 20 S-TWIN for probing the morphology, particle size and size distribution of NPs. EDX spectra were obtained using a LEO 1530 scanning electron microscope for studying the ratio of elements in the resulting metal alloy NPs. Magnetic properties of the as-prepared NPs were investigated at room temperature and 5 K using a Quantum Design system with a vibrating sample magnetometer (VSM), with an applied field of up to 7 T.

Acknowledgements

We acknowledge the financial support from the National Natural Science Foundation of China (Grant No.: 61307030 and 51373145), Hong Kong Research Grants Council (HKBU203312), Areas of Excellence Scheme, University Grants Committee of HKSAR (AoE/P-03/08), Science, Technology and Innovation Committee of Shenzhen Municipality (JCYJ 20140419130507116), Hong Kong Baptist University (FRG2/13-14/083) and Hundred Talents Program of Shanxi Province. The work was also supported by Partner State Key Laboratory of Environmental and Biological Analysis (SKLP-14-15-P011) and Strategic Development Fund of HKBU. Q. Dong

also thanks the financial support from the Program for the Outstanding Innovative Teams of Higher Learning Institutions of Shanxi (OIT), Fund Program for the Scientific Activities of Selected Returned Overseas Professionals in Shanxi Province, the Natural Science Foundation for Young Scientists of Shanxi Province, China (Grant No. 2014021019-2), and the Outstanding Young Scholars Cultivating Program, Research Project Supported by Shanxi Scholarship Council of China (Grant No. 2014-02). W. Qu thanks the financial support from Datong City Science and Technology Research Projects and the Doctoral Scientific Research Foundation of Shanxi Datong University. Y. H. Lo gratefully acknowledges the financial support from the National Science Council of Taiwan (NSC 102-2113-M-845-001) and the project of the specific research fields in the University of Taipei, Taiwan.

Graphical abstract

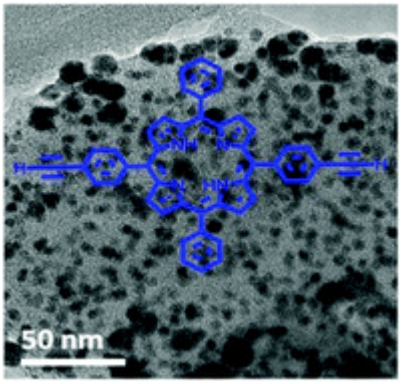

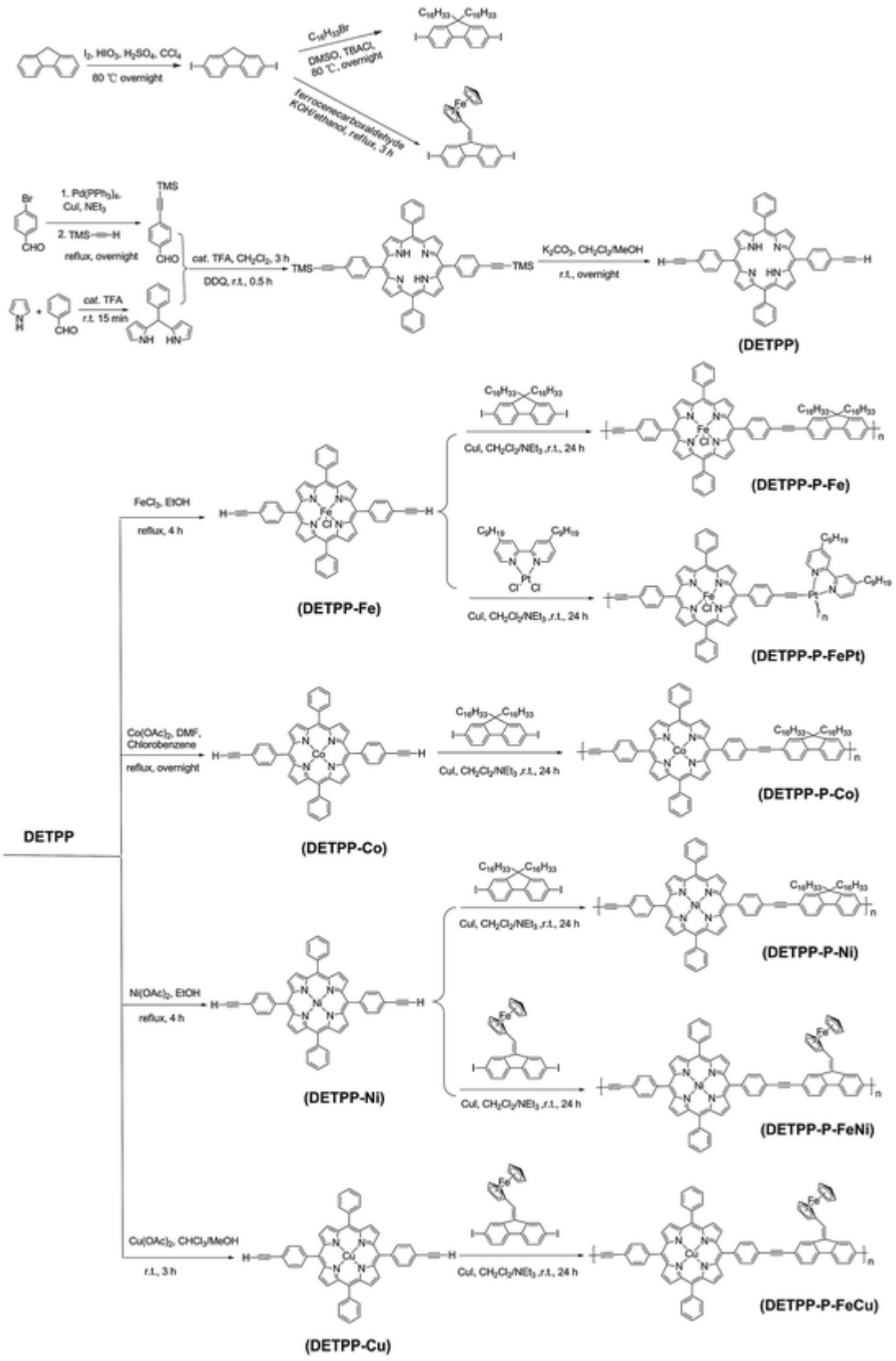

Scheme 1 General synthetic routes for the porphyrin-based metallopolymers.

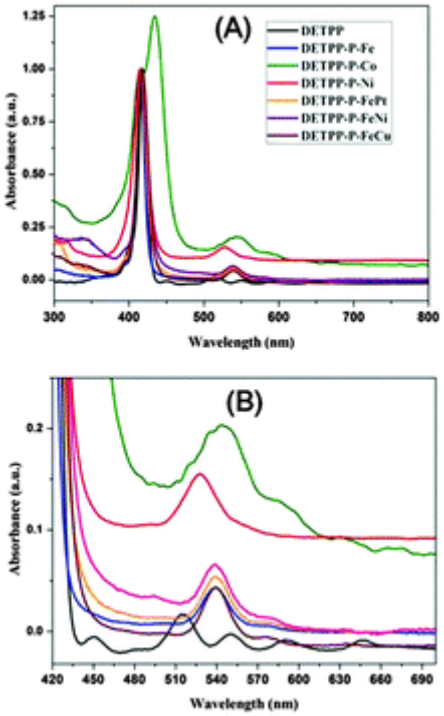

Fig. 1 (a) Normalized absorption spectra of the as-synthesized porphyrin-based metallopolymers and (b) enlarged absorption spectra from 420 nm to 700 nm.

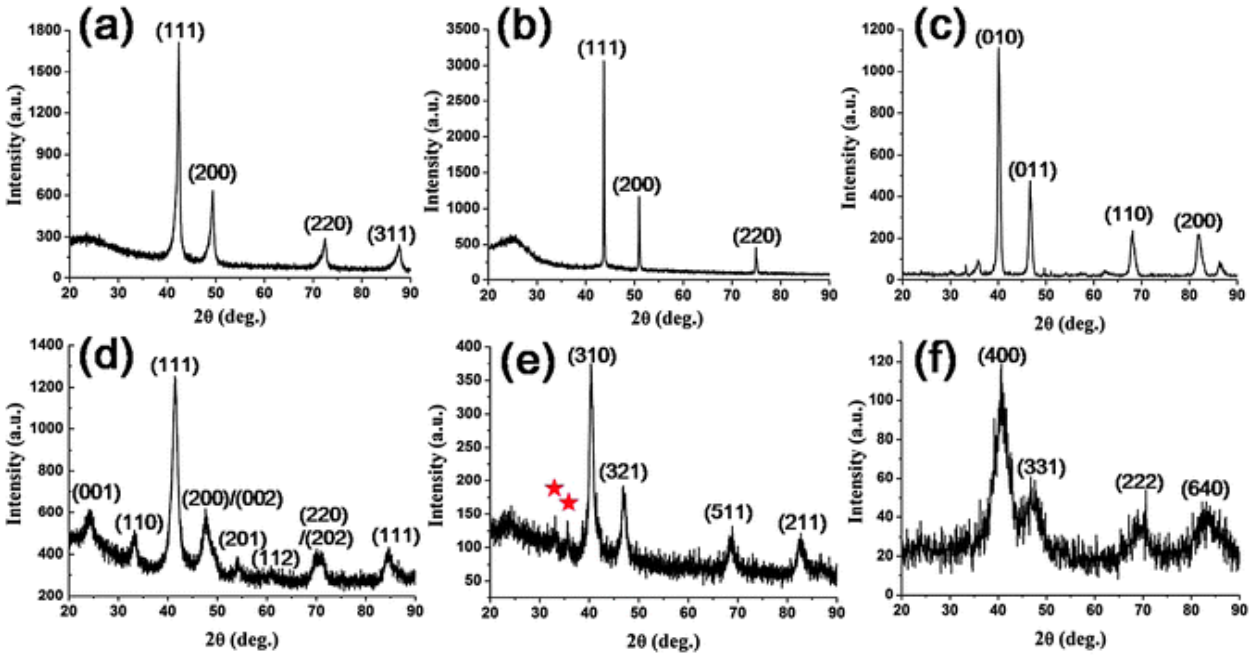

Fig. 2 XRD spectra of the as-prepared NPs from pyrolysis of porphyrin-based metallopolymers: (a) NP-Fe, (b) NP-Co, (c) NP-Ni, (d) NP-FePt, (e) NP-FeNi and (f) NP-FeCu.

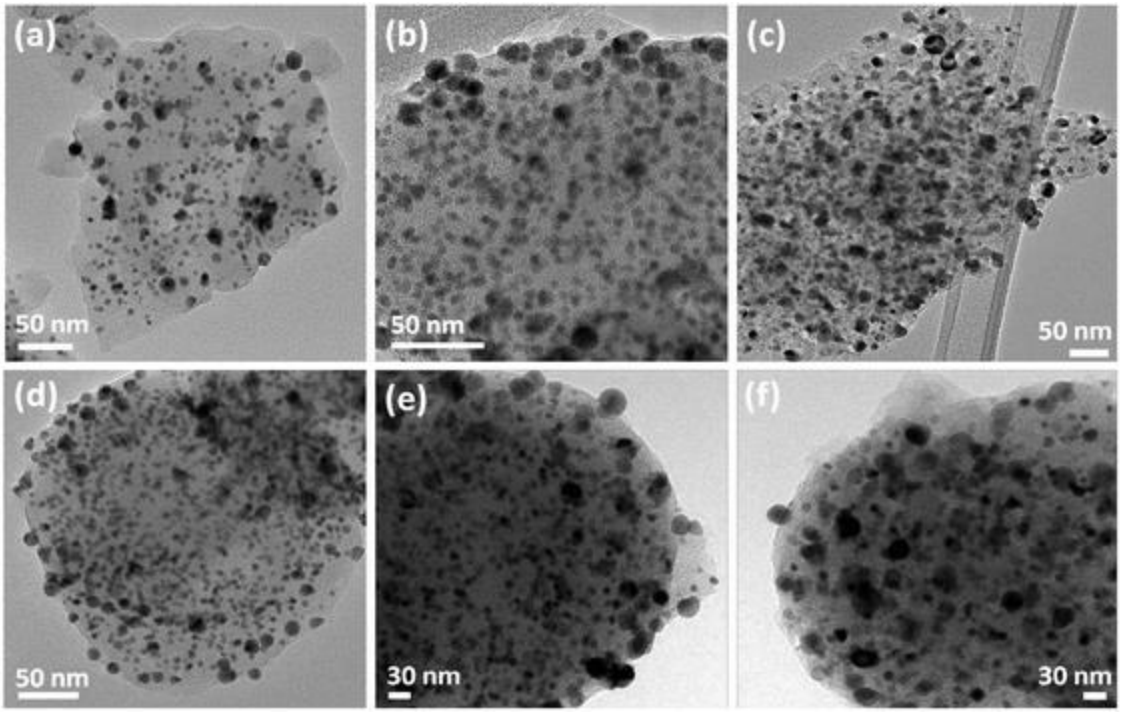

Fig. 3 TEM and high-resolution TEM (HRTEM) images of (a) NP-Fe, (b) NP-Co, (c) NP-Ni, (d) NP-FePt, (e) NP-FeNi and (f) NP-FeCu.

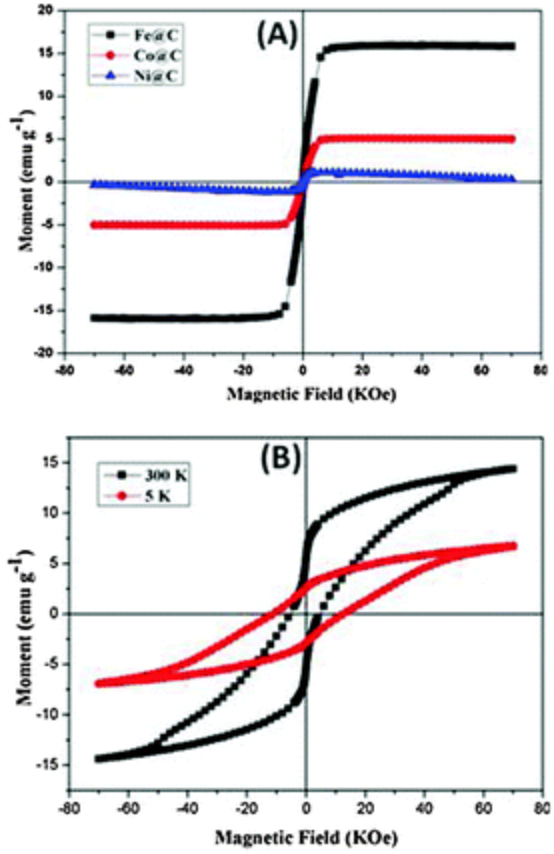

Fig. 4 Hysteresis loops of the as-prepared Fe-, Co-, and Ni-NPs measured at 300 K (A) and $L1_0$ FePt NPs measured at 300 K and 5 K (B).

Reference

1 V. Bellas and M. Rehahn, Angew. Chem., Int. Ed., 2007, 46, 5082.

2 G. R. Whittell, M. D. Hager, U. S. Schubert and I. Manners, Nat. Mater., 2011, 10, 176.

3 K. A. Williams, A. J. Boydston and C. W. Bielawski, Chem. Soc. Rev., 2007, 36, 729.

4 B. J. Holliday and T. M. Swager, Chem. Commun., 2005, 23.

5 W. Y. Wong and C. L. Ho, Coord. Chem. Rev., 2006, 250, 2627.

6 W. Y. Wong, X. Z. Wang, Z. He, A. B. Djurisˇic´, C. T. Yip, K. Y. Cheung, H. Wang, C. S. K. Mak and W. K. Chan, Nat. Mater., 2007, 6, 521.

7 M. L. Mejı´a, K. Agapiou, X. Yang and B. J. Holliday, J. Am. Chem. Soc., 2009, 131, 18196.

8 M. L. Mejı´a, G. Reeske and B. J. Holliday, Chem. Commun., 2010, 46, 5355.

9 P. Bertoncello and R. J. Forster, Biosens. Bioelectron., 2009, 24, 3191.

10 W.-Y. Wong, Dalton Trans., 2007, 4495.

11 M. A. Rawashdeh-Omary, J. M. Lo´pez-de-Luzuriaga, M. D. Rashdan, O. Elbjeirami, M. Monge, M. Rodriguez-Castillo and A. Laguna, J. Am. Chem. Soc., 2009, 131, 3284.

12 J. B. Gilroy, S. K. Patra, J. M. Mitchels, M. A. Winnik and I. Manners, Angew. Chem., Int. Ed., 2011, 50, 5851.

13 K. Liu, S. B. Clendenning, L. Friebe, W. Y. Chan, X. Zhu, M. R. Freeman, G. C. Yang, C. M. Yip, D. Grozea, Z. H. Lu and I. Manners, Chem. Mater., 2006, 18, 2591.

14 S. B. Clendenning, S. Aouba, M. S. Rayat, D. Grozea, J. B. Sorge, Z. H. Lu, C. M. Yip, M. R. Freeman, H. E. Ruda and I. Manners, Adv. Mater., 2004, 16, 215.

15 S. B. Clendenning, S. Han, N. Coombs, C. Paquet, M. S. Rayat, D. Grozea, P. M. Brodersen, R. N. S. Sodhi, C. M. Yip, Z. H. Lu and I. Manners, Adv. Mater., 2004, 16, 291.

16 J. B. Shi, C. J. W. Jim, F. Mahtab, J. Z. Liu, J. W. Y. Lam, H. H. Y. Sung, I. D. Williams, Y. P. Dong and B. Z. Tang, Macromolecules, 2010, 43, 680.

17 J. Liu, J. W. Y. Lam, M. Ha¨ussler, A. Qin and B. Z. Tang, J. Inorg. Organomet. Polym. Mater., 2009, 19, 133.

18 W. Z. Yuan, J. Z. Sun, J. Z. Liu, Y. Dong, Z. Li, H. P. Xu, A. Qin, M. Ha¨ussler, J. K. Jin, Q. Zheng and B. Z. Tang, J. Phys. Chem. B, 2008, 112, 8896.

19 K. Liu, C. L. Ho, S. Aouba, Y. Q. Zhao, Z. H. Lu, S. Petrov, N. Coombs, P. Dube, H. E. Ruda, W. Y. Wong and I. Manners, Angew. Chem., Int. Ed., 2008, 47, 1255.

20 Q. C. Dong, G. J. Li, C. L. Ho, M. Faisal, C. W. Leung, P. W. T. Pong, K. Liu, B. Z. Tang, I. Manners and W. Y. Wong, Adv. Mater., 2012, 24, 1034.

21 Q. C. Dong, G. J. Li, H. Wang, P. W. T. Pong, C. W. Leung, I. Manners, C. L. Ho, H. Li and W. Y. Wong, J. Mater. Chem. C, 2015, 3, 734.

22 S. Fu, X. Zhu, G. Zhou, W. Y. Wong, C. Ye, W. K. Wong and Z. Y. Li, Eur. J. Inorg. Chem., 2007, 2004.

23 O. S. Finikova, P. Chen, Z. Ou, K. M. Kadish and S. A. Vinogradov, J. Photochem. Photobiol., A, 2008, 198, 75.

24 N. Araki, Y. Amao, T. Funabiki, M. Kamitakahara, C. Ohtsuki, K. Mitsuo, K. Asai, M. Obata and S. Yano, Photochem. Photobiol. Sci., 2007, 6, 794.

25 F. L. Jiang, W. K. Wong, X. J. Zhu, G. J. Zhou, W. Y. Wong, P. L. Wu, H. L. Tam, K. W. Cheah, C. Ye and Y. Liu, Eur. J. Inorg. Chem., 2007, 3365.

26 W. Maes, J. Vanderhaeghen, S. Smeets, C. V. Asokan, L. M. V. Renterghem, F. E. Du Prez, M. Smet and W. Dehaen, J. Org. Chem., 2006, 71, 2987.

27 I. V. Sazanovich, A. Balakumar, K. Muthukumaran, E. Hindin, C. Kirmaier, J. R. Diers, J. S. Lindsey, D. F. Bocian and D. Holten, Inorg. Chem., 2003, 42, 6616.

28 L. Liu, D. Fortin and P. D. Harvey, Inorg. Chem., 2009, 48, 5891.

29 H. L. Anderson, Chem. Commun., 1999, 2323.

30 T. Yamamoto, N. Fukushima, H. Nakajima, T. Maruyama and I. Yammaguchi, Macromolecules, 2000, 33, 5988.

31 T. J. Klemmer, N. Shukla, C. Liu, X. W. Wu, E. B. Svedberg, O. Mryasov, R. W. Chantrell, D. Weller, M. Tanase and D. E. Laughlin, Appl. Phys. Lett., 2002, 81, 2220.

32 K. L. McNerny, Y. Kim, D. E. Laughlin and M. E. McHenry, J. Appl. Phys., 2010, 107(9(A)), 312.

33 X. G. Liu, D. Y. Geng, C. J. Choi, J. C. Kim and Z. D. Zhang, J. Nanopart. Res., 2009, 11, 2097.

34 T. Komeda, H. Isshiki, J. Liu, Y.-F. Zhang, N. Lorente, K. Katoh, B. K. Breedlove and M. Yamashita, Nat. Commun., 2011, 2, 217–385.

35 Q. C. Dong, G. J. Li, C. W. Leung, P. W. T. Pong, I. Manners and W. Y. Wong, Adv. Funct. Mater., 2014, 24, 857.